

## Study on P-V Curve and V-Q Curve of an Unbalanced Three-Phase System with Different Static Loads

**Abstract** P-V curve and V-Q curve (often term as Q-V curve) are widely used for planning and operation studies. The P-V curve and V-Q curve of an unbalanced three-phase system, unlike the balanced three-phase system, may not have similar loading margin (LM) and reactive power margin (RPM) on each phase. Therefore, DigSILENT Programming Language (DPL) has been used to study the maximum loading point (MLP), critical point (CP), and also minimum reactive power point (MRPP) on each phase of an unbalanced three-phase system with different static loads. The tracing direction of P-V curve of each phase and the LM and RPM of each phase obtained from the P-V curve and V-Q curve for different static loads are also discussed. On top of that, continuation power flow (CPF) has become a common method to study the MLP. Hence, a simple 2-bus balanced three-phase system is used to validate the result obtained from the DigSILENT with CPF method.

**Streszczenie.** Krzywe P-V i V-Q w systemie trójfazowym niezrównoważonym mogą nie mieć tego samego marginesu obciążenia LM i marginesu mocy biernej RPM w każdej z faz. Zastosowano język programowania DigSILENT do określenia maksymalnego punktu obciążenia MLP, punktu krytycznego CP i punktu minimalnej mocy biernej MRPP. Analiza krzywych P-V i V-Q w niezrównoważonym układzie trójfazowym o różnych obciążeniach statycznych

**Keywords:** Continuation power flow (CPF), Critical point (CP), DigSILENT, Loading margin (LM), Static load, V-Q curve.

**Słowa kluczowe:** margines obciążenia LM system trójfazowego, krzywa V-Q, krzywa P-V

### Introduction

Voltage stability problems have been recognized as the main causes for blackouts throughout the world in the recent past. The limited expansion of transmission and distribution system due to cost and environmental issues, and continuous increase in the load demand lead the existing power system operate near to voltage stability limit [1]. Hence, an accurate knowledge of how close the actual system's operating point is from the voltage stability limit is crucial to operators [2].

In the recent years, several research works have been carried out on unbalanced three-phase system particularly related to voltage stability. In [3] multiple solutions at the neutral points are presented and [4] extends by proposing two P-V curve for each phase. In [5] voltage stability analysis using P-V curves (using loading factor) of constant power load has been presented and [6] study with voltage regulation of transformers with different fixed tap ratios, and distributed generation using CPF. On the other hand, STATCOM compensation under different contingencies is studied with constant power load [7]. In [8] maximum three-phase active power and also contribution to the maximum three-phase active power due to three phases against different power factors are presented for different load characteristics using optimal power flow.

In spite of the performed research work on this area, there is a lack of studies on the tracing direction of P-V curve, MLP and CP (which is an important boundary of voltage stability feasible region) of each phase for different static loads. Also, to the best knowledge of the author, MRPP of each phase has not been studied for an unbalanced three-phase system. Hence, this paper is mainly address such a study using the proposed P-V script and V-Q script. In this paper, the studies are carried out using 8-bus unbalanced three-phase system by means of DigSILENT/PowerFactory Version 14.0 software. Results obtained from the P-V curve (LM) and V-Q curve (RPM) of each phase are also compared and discussed. Since CPF method predicts an exact MLP, hence, a simple 2-bus balanced three-phase system is used for validation such that similar MLP is also obtained from DigSILENT.

The paper is organized as follows. Section II and III present static load modelling and test distribution system, respectively. The critical point (CP) and nose point (or MLP) are discussed in Section IV. Definition and brief descriptions

on the V-Q curve are presented in Section V. Determination on MLP and CP is explained in Section VI. Flow chart of the proposed P-V script and V-Q script are presented in Section VII. Validation on DigSILENT result is presented in Section VIII. The results and discussions are presented and discussed in Section IX. Finally, conclusion is presented in Section X.

### Static Load Modelling

Static load consists of constant power, constant current and constant impedance load. They are generally modelled as active power and reactive power. Their respective characteristics are represented by exponential model, as shown in (1) and (2), where  $P$  and  $Q$  are active power and reactive power of the load respectively at the considered bus when the voltage magnitude is  $V$ . The subscript 0 indicates initial operating conditions. The exponents "a" and "b" can be 0, 1, or 2, to represent constant power, constant current, or constant impedance characteristics, respectively [9].

$$(1) \quad P = P_o \left( \frac{V}{V_o} \right)^a$$

$$(2) \quad Q = Q_o \left( \frac{V}{V_o} \right)^b$$

### Test Distribution System

A single line diagram of the distribution network, as shown in the Appendix, is used for the analysis. This system has single phase load connected to single phase line, and two single phase loads and three single phase loads connected to the three phase lines. All these single phase loads are connected phase-to-neutral/ground. The single phase and three phase overhead line configuration are 303 and 300 respectively which can be obtained in [10]. The data of the loads is also shown in the Appendix.

### Critical Point and Nose Point

Voltage collapse is associated with saddle-node bifurcation (SNB) where system equilibrium disappears as system parameters, mostly system load, changes [11]. Some earlier works have been presented that the nose point (or MLP) of the P-V curve is the voltage collapse (or critical) point. However, the actual voltage collapse point is the SNB of the bifurcation curve and the SNB (or critical) point coincides with the nose point only if the load is

constant power. Otherwise, the SNB point will not coincide with the nose point of the P-V curve, but to the other part of the P-V curve (such as B'' on the P-V curve in Fig. 1) [12], [13]. In that case, the voltage collapse is no longer a nose point but at point B on the P-V curve.

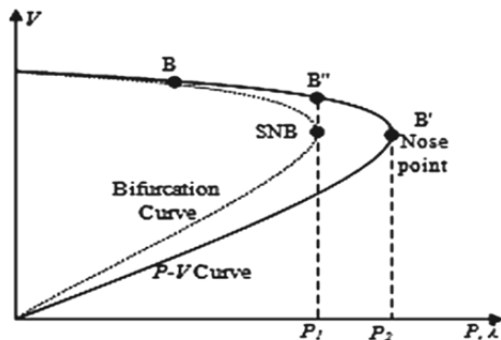


Fig. 1. Bifurcation curve and P-V curve of negative exponential load [14]

### V-Q Curve

V-Q curve (often term as Q-V curve), on the other hand, is used to determine the RPM of a system. V-Q curve analysis is usually performed in conjunction with P-V curve. With this curve, it is possible for the operator to know how much reactive power can be added to the weakest bus before reaching the voltage stability limit. The voltage stability limit is reached when the sensitivity  $dQ/dV$  is zero as shown in Fig. 2. The RPM is the MVAR distance from the operating point to the bottom of the curve. If the operating point is on the right side of the curve indicates that system is stable. However, if the operating point is on the left side of the curve, the system is diagnosed to be in unstable condition [2], [14].

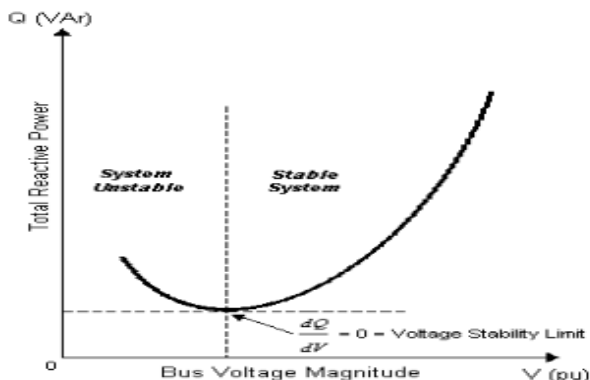


Fig. 2. Typical V-Q curve [14]

### Determination on MLP and CP

CPF determines the bifurcation or point of collapse by increasing the bifurcation (or loading) parameter as per (3) and (4).

$$(3) \quad P_{di} = \lambda_f P_{di,0}$$

$$(4) \quad Q_{di} = \lambda_f Q_{di,0}$$

where  $P_{di}$  and  $Q_{di}$  are active power and reactive power of the load at the  $i$ th bus, respectively. The subscript 0 indicates at initial operating condition and  $\lambda_f$  is the bifurcation (or loading) parameter [15]. By plotting the P-V curve using loading factor, the MLP can be determined. In the case of balanced three-phase system, the representation of P-V curve (using loading factor) provides accurate information on CP. However, for unbalanced three-phase system, it is not necessarily all the three phases will

collapse at the same time, particularly for voltage dependent loads as their actual MLP and CP are different.

On the other hand, the SNB (or critical) point does not exist for a constant impedance load but exist for a constant current load [13]. This is true if there is only one load in the system. In reality, the SNB also exists for constant impedance load as distribution system consists of many and different types of loads.

### Flow Chart

DigSILENT Programming Language (DPL) is used to study the LM and RPM of an unbalanced three-phase system. Also, another advantage of the proposed P-V script is that it can be used for all types of load characteristics i.e. voltage independent load and voltage dependent loads. The flow chart of P-V script and V-Q script are shown in Fig. 3 and Fig. 4, respectively.

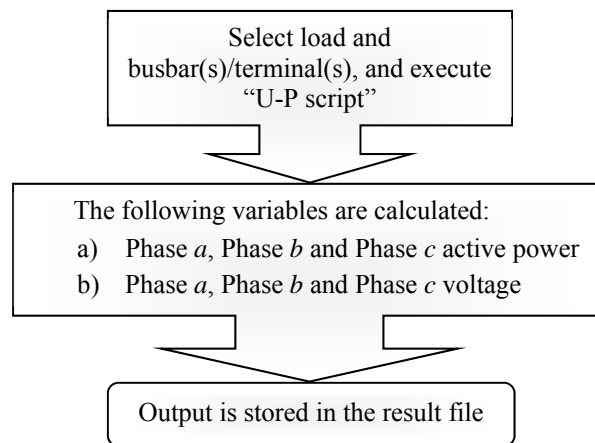


Fig. 3. Flow Chart of P-V script

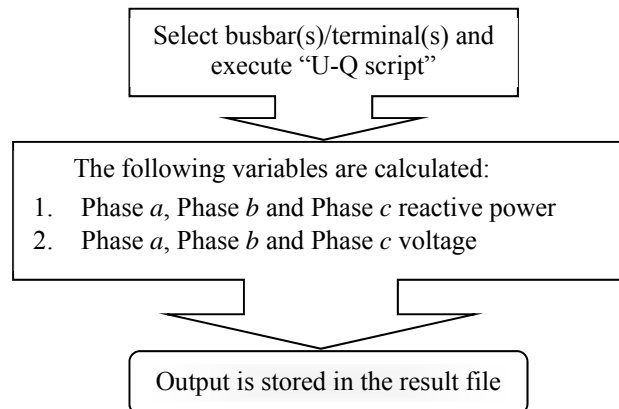


Fig. 4. Flow Chart of V-Q script

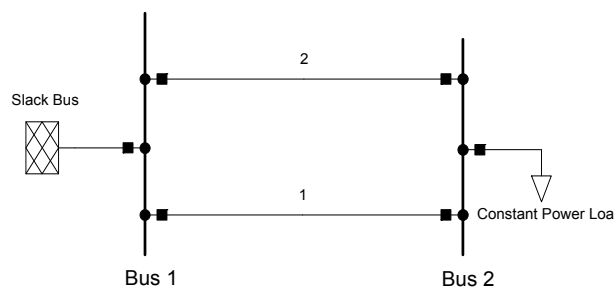


Fig. 5. 2-bus balanced three-phase system

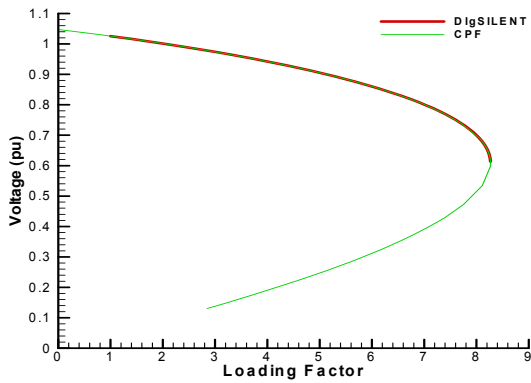


Fig.6. P-V curve of DlgSILENT and PSAT

### Results Validation

Figure 5 shows 2-bus balanced three-phase system which is used for validation on DlgSILENT result with CPF method. The data of the system is shown in the Appendix. CPF is performed using power system analysis toolbox (PSAT) software package [16]. In DlgSILENT, the scaling factor also known as loading factor starts from one (from initial loading) as compared to PSAT where it starts from zero. Figure 6 shows that the MLP obtained from DlgSILENT show an agreement with that of PSAT.

### Results and Discussions

The voltage stability of the system is analyzed by considering three different buses i.e. bus 4, bus 6 and bus 7. In base case, constant power load, constant current load and constant impedance load are the corresponding load characteristics, and these loads have a balanced loading. Three different cases are analyzed.

- Individual increment of three different static loads (balanced loads).
- Individual increment of three different static loads (unbalanced loads).
- Individual increment of voltage dependent loads (unbalanced loads).

Unbalanced loading of a load for case (b) is created by reducing the load on phase *a* and phase *b* by 20% and 10%, respectively. For case (c), the load on phase *a* and phase *b* are reduced by 30% and 20%, respectively. However, the load on phase *c* remains unchanged.

#### A. Case a: Individual Increment of Three Different Static Loads (Balanced Loads)

The P-V curves of bus 4, bus 6 and bus 7 are shown in Fig. 7 to Fig. 9, respectively. The numerical values at MLP and CP for the respective buses are shown in the Table I-Table III. At MLP and CP, both the active power and voltage of each phase are presented. While V-Q curves of bus 4, bus 6 and bus 7 are shown in the Fig. 10 to Fig. 12, respectively. The MRPP of each phase for the respective buses is also shown in the Table IV-Table VI. At MRPP, both the reactive power and voltage of each phase are presented.

Table 1. MLP and CP at Bus 4

Numerical Values			
Phases	Phase A	Phase B	Phase C
MLP (MW)	1.471340	1.471340	1.471340
MLP (Volt.,pu)	0.610127	0.617706	0.534455
CP (MW)	1.471340	1.471340	1.471340
CP (Volt.,pu)	0.610127	0.617706	0.534455

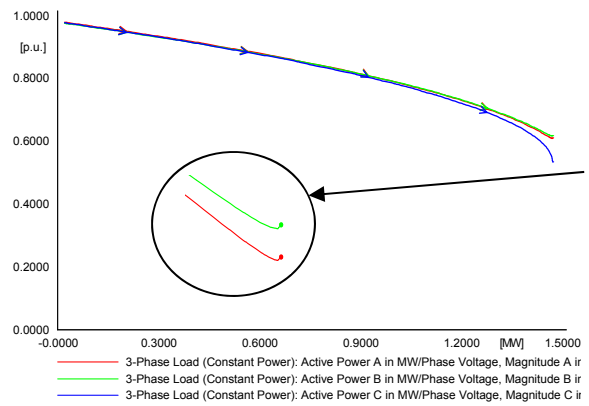


Fig.7. P-V curves at bus 4 (Constant power load)

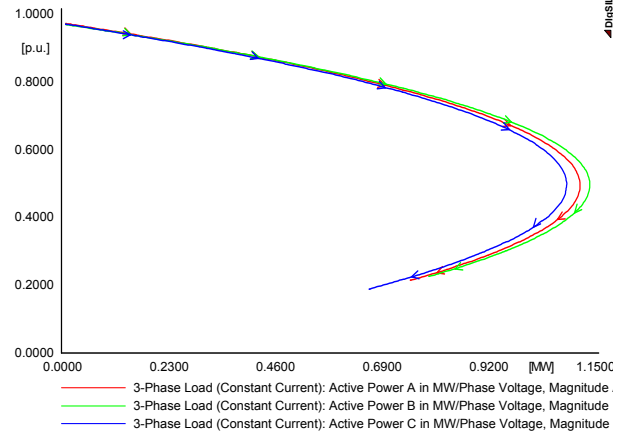


Fig.8. P-V curves at bus 6 (Constant current load)

Table 2. MLP and CP at Bus 6

Numerical Values			
Phases	Phase A	Phase B	Phase C
MLP (MW)	1.118854	1.140018	1.090015
MLP (Volt.,pu)	0.493559	0.494849	0.497002
CP (MW)	0.752041	0.792521	0.663553
CP (Volt.,pu)	0.213073	0.224542	0.187996

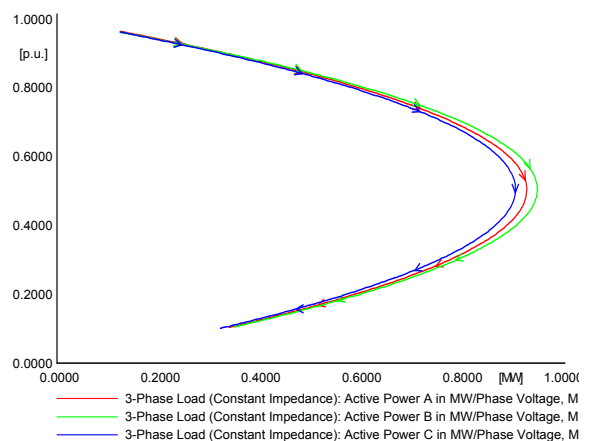


Fig.9. P-V curves at bus 7 (Constant impedance load)

Table 3. MLP and CP at Bus 7

Numerical Values			
Phases	Phase A	Phase B	Phase C
MLP (MW)	0.932004	0.952897	0.909490
MLP (Volt.,pu)	0.503845	0.509462	0.507367
CP (MW)	0.342217	0.351174	0.323602
CP (Volt.,pu)	0.103620	0.104967	0.100762

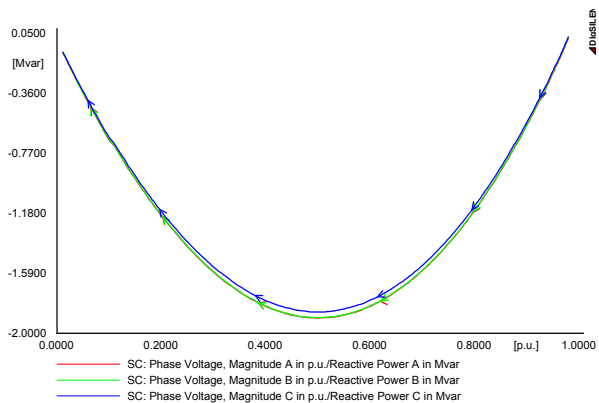


Fig.10. V-Q curves at bus 4 (Constant power load)

Table 4.MRPP and CV at Bus 4

Numerical Values			
Phases	Phase A	Phase B	Phase C
MRPP (MVar)	-1.896496	-1.895155	-1.855485
MRPP (Volt.,pu)	0.499128	0.499122	0.499062

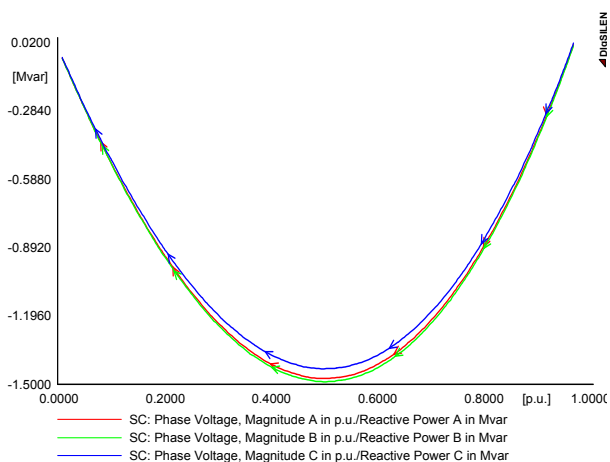


Fig.11. V-Q curves at bus 6 (Constant current load)

Table 5.MRPP and CV at Bus 6

Numerical Values			
Phases	Phase A	Phase B	Phase C
MRPP (MVar)	-1.474766	-1.488833	-1.431680
MRPP (Volt.,pu)	0.500754	0.500765	0.500687

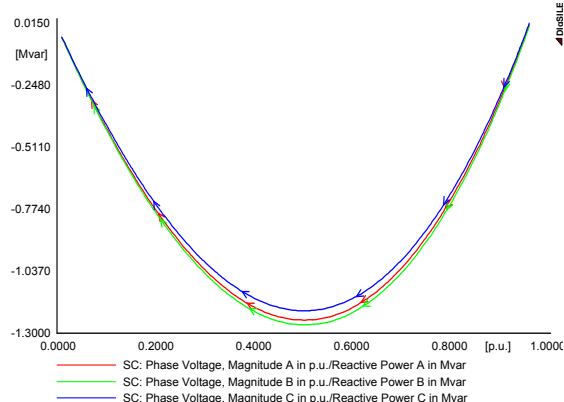


Fig.12. V-Q curves at bus 7 (Constant impedance load)

According to Fig. 7 (Table I) voltage and active power at MLP on each phase is similar to that of CP on each phase. This shows that the MLP and CP are coincide to each other for this type of load. Also, each phase has similar active power at MLP and CP due to the independency with voltage and balanced loading. Due to that, the three phases will collapse at the same time. The tracing direction of phase a

and phase b of the P-V curves, on the other hand, show anti-clockwise direction. This reflects that the upper portion of the phase a and phase b curve are unstable system while the lower portion corresponds to the stable system.

Table 5.MRPP and CV at Bus 7

Numerical Values			
Phases	Phase A	Phase B	Phase C
MRPP (MVar)	-1.245020	-1.265446	-1.205349
MRPP (Volt.,pu)	0.504361	0.504378	0.504299

Despite that, Fig. 8 (Table II) and Fig. 9 (Table III) show that there are SNB (or critical) points for pure voltage dependent loads i.e. constant current load and constant impedance load, respectively. It can be seen that, in Fig. 8 (Table II) and Fig. 9 (Table III), MLP and CP on each phase are not coincide to each other. The CP of each phase is actually found on the lower part of the curves reflecting that the system can be stable on the lower part of the curves. It is also shown that, in Fig. 9 (Table III), phase a and phase b will collapse at the same time as the active power at CP for both phases is almost similar. Besides that, the tracing direction of P-V curves of voltage dependent loads is similar to the tracing direction of P-V curve of a balanced three-phase system i.e. clockwise direction.

On the other hand, the existence of LM of each phase has been proved with V-Q curve where each phase has its own RPM as shown in Fig. 10 (Table IV) to Fig. 12 (Table VI). The LM and RPM of each phase are as follows:

Bus 4 : P margin of phase  $a = b = c$   
Q margin of phase  $a \approx b > c$

Bus 6 and 7: P margin of phase  $b > a > c$   
Q margin of phase  $b > a > c$

Similar LM on each phase but different RPM on some phases is because V-Q curve method is artificial, involving stress at a single bus for local area evaluation and also the allowable power loading or interface flow is not directly given. P-V curve method, on the other hand, is more realistically stress a power transfer path, allowing more global evaluation [17].

### B. Case b: Individual Increment of Three Different Static Loads (Unbalanced Loads)

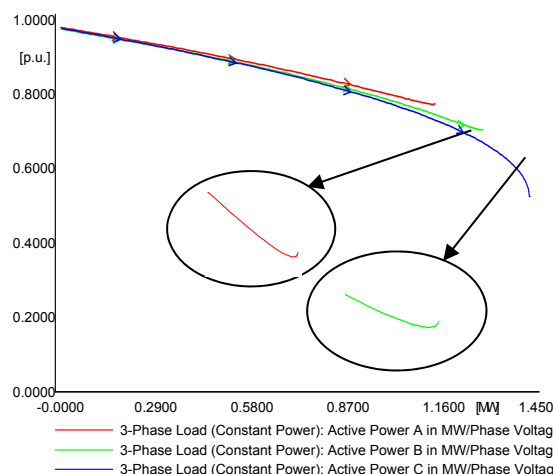


Fig.13. P-V curves at bus 4 (Constant power load)

It is found that, when the load is unbalanced, interesting observation is seen for unbalanced constant power load. It shows that, in Fig 13 (Table VII), the three phases will not collapse at the same time. In fact, phase a will collapse first followed by phase b and then phase c. The tracing direction of P-V curves is found to be similar as in previous case

where phase *a* and phase *b* have anti-clockwise direction and also MLP and CP of each phase are coincide with each other. Fig. 14 and Fig. 15, on the other hand, are also show similar observation as in previous case for tracing direction where all the three phase have clockwise direction and CP of each phase is found on the lower portion of the curves. However, it is found that CP particularly for phase *a* of Fig. 14 (Table VIII) is getting nearer to their MLP as compared to Fig. 15 (Table IX). On top of that, even though the active power at MLP of phase *a* and phase *b* of Fig 15 (Table IX) is almost similar but not necessarily they will collapse at the same time due to the different active power at CP. This indicates that collapse of a phase is determined by CP of a phase and not by MLP of a phase. The RPM of each phase at each bus, on the other hand, has similar observations as in previous case.

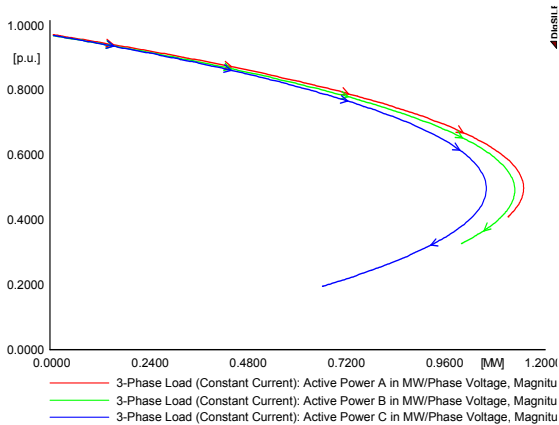


Fig. 14. P-V curves at bus 6 (Constant current load)

Table 6. MLP and CP at Bus 4

Numerical Values			
Phases	Phase A	Phase B	Phase C
MLP (MW)	1.145456	1.288639	1.431754
MLP (Volt.,pu)	0.773746	0.705335	0.525698
CP (MW)	1.145456	1.288639	1.431754
CP (Volt.,pu)	0.773746	0.705335	0.525698

Table 7. MLP and CP at Bus 6

Numerical Values			
Phases	Phase A	Phase B	Phase C
MLP (MW)	1.156433	1.134834	1.065450
MLP (Volt.,pu)	0.497979	0.490435	0.492004
CP (MW)	1.118420	1.004359	0.664749
CP (Volt.,pu)	0.408909	0.326406	0.194431

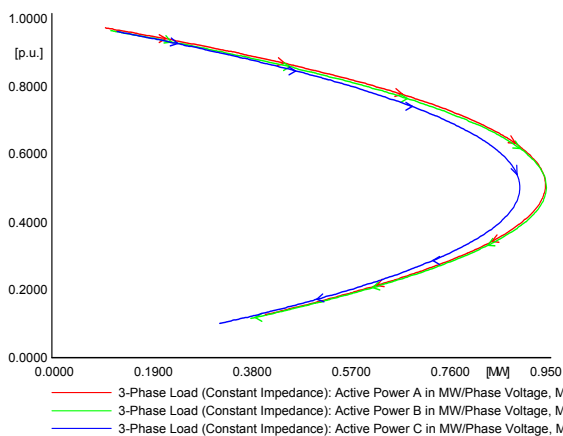


Fig. 15. P-V curves at bus 7 (Constant impedance load)

Table 8. MLP and CP at Bus 7

Numerical Values			
Phases	Phase A	Phase B	Phase C
MLP (MW)	0.946803	0.948810	0.897749
MLP (Volt.,pu)	0.506496	0.501088	0.505921
CP (MW)	0.409234	0.381674	0.322232
CP (Volt.,pu)	0.126739	0.115397	0.100589

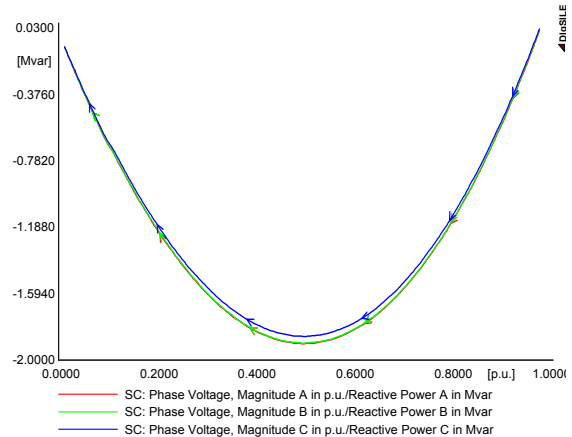


Fig. 16. P-V curves at bus 4 (Constant power load)

Table 9. MRPP and CV at Bus 4

Numerical Values			
Phases	Phase A	Phase B	Phase C
MRPP (MVar)	-1.900157	-1.897127	-1.855899
MRPP (Volt.,pu)	0.499814	0.499808	0.499745

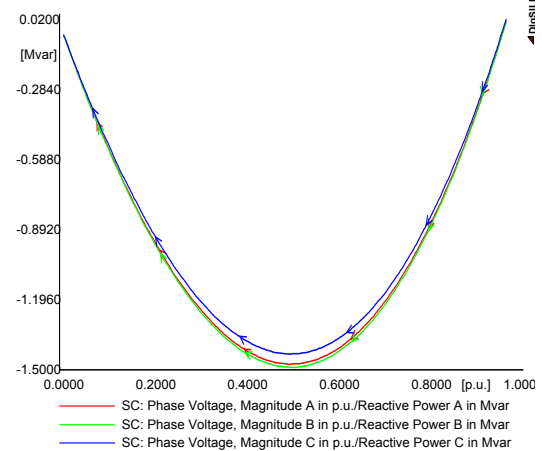


Fig. 17. P-V curves at bus 6 (Constant current load)

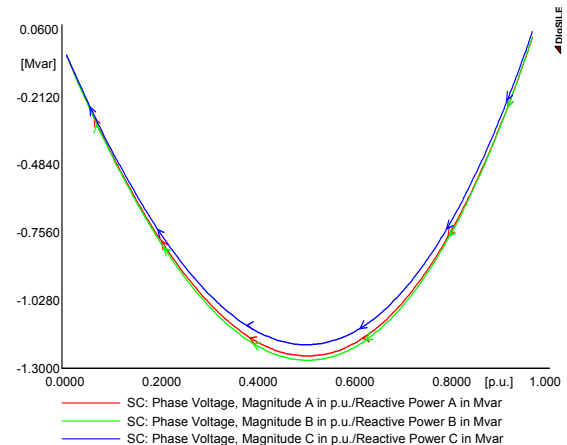


Fig. 18. P-V curves at bus 7 (Constant impedance load)

Table 10.MRPP and CV at Bus 6

Numerical Values			
Phases	Phase A	Phase B	Phase C
MRPP (MVA <sub>r</sub> )	-1.475620	-1.489313	-1.431813
MRPP (Volt.,pu)	0.501190	0.501201	0.501122

Table 11.MRPP and CV at Bus 7

Numerical Values			
Phases	Phase A	Phase B	Phase C
MRPP (MVA <sub>r</sub> )	-1.251654	-1.269105	-1.206363
MRPP (Volt.,pu)	0.512400	0.512417	0.502334

C. Case c: Individual Increment of Voltage Dependent Loads (Unbalanced Loads)

In this case, only P-V curves of constant current load and constant impedance load are presented. It is because similar observations are obtained as in previous case for constant power load, and also for V-Q curves at each bus. It is shown that, in Fig. 19 (Table XIII), the MLP and CP of phase a are coincide with each other as they have similar active power and voltage at MLP and CP. The CP of phase b is getting closer to its MLP whereas the CP of phase c is far away from its MLP. The CP of both these two phases is found on the lower part of the curve. On the other hand, as shown in Fig. 20 (Table XIV), similar observations are seen as in previous case when the same unbalanced is introduced to the constant impedance load i.e. the MLP and CP of each phase do not coincide with each other. This is mainly due to its characteristics where the constant current load power is directly proportional to the voltage magnitude, while constant impedance load power is directly proportional to the square to the voltage magnitude.

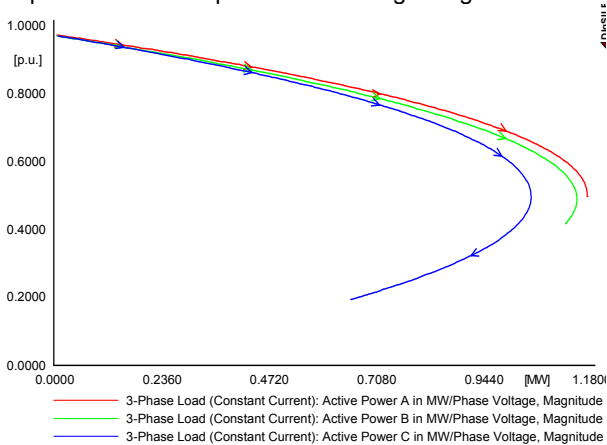


Fig.19. P-V curves at bus 6 (Constant current load)

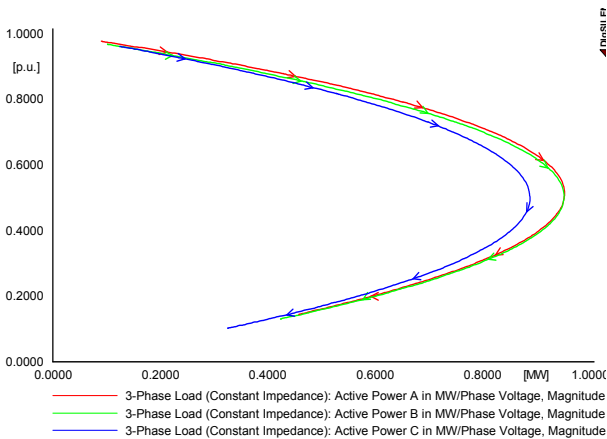


Fig.20. P-V curves at bus 7 (Constant impedance load)

Table 12.MLP and CP at Bus 6

Numerical Values			
Phases	Phase A	Phase B	Phase C
MLP (MW)	1.172229	1.149892	1.049151
MLP (Volt.,pu)	0.501987	0.488953	0.492868
CP (MW)	1.172068	1.124778	0.653166
CP (Volt.,pu)	0.496432	0.416852	0.193655

Table 13.MLP and CP at Bus 7

Numerical Values			
Phases	Phase A	Phase B	Phase C
MLP (MW)	0.953138	0.951979	0.888511
MLP (Volt.,pu)	0.512603	0.499614	0.497336
CP (MW)	0.458299	0.423758	0.325395
CP (Volt.,pu)	0.144607	0.130070	0.101946

Conclusions

This paper presented study on the tracing direction of P-V curve, MLP, CP and also MRPP of each phase for different static loads under balanced and unbalanced loading using the proposed P-V and V-Q scripts. The DlgSILENT result is also validated with CPF result using a 2-bus balanced three-phase system. The DlgSILENT result shows an agreement with CPF method. The SNB (or critical) point also exists for pure voltage dependent loads (constant current load and constant impedance load).

In general, depending on the types of loads and balanced or unbalanced loading, each phase has its own MLP and CP. In fact, the collapse of a phase can be determined only by the actual CP of a phase and not MLP of a phase. For constant power load, the MLP and CP of each phase coincide with each other. On the other hand, for voltage dependent loads, the MLP and CP of each phase may or may not coincide with each other. Under balanced loading, MLP and CP do not coincide with each other and CP of each phase is found on the lower part of the curve. In this case, the system can be stable on the lower part of the curve. However, under unbalanced loading, the CP of some phases may get closer to their MLP. Depending on the unbalanced loading level, the MLP and CP of one of the three phases will coincide with each other. This can be easily seen for constant current load as compared to constant impedance load due to their characteristic.

Despite that, the tracing direction of P-V curves of voltage dependent loads is always clockwise regardless the load is balanced or unbalanced. However, the tracing direction of some phases of P-V curves of constant power load will not be in clockwise direction. At least one phase will have anti-clockwise direction. In such case, the upper portion of the curve is corresponding to an unstable system while lower portion corresponds to a stable system.

Different LM on each phase shows that there is also a different RPM on each phase. However, dissimilarities between the LM and RPM of some phases may be observed. This is because V-Q curve method, unlike the P-V curve method, is artificial and it does not stress a power transfer path. Also, the allowable power loading or interface flow is not directly given in the V-Q curve method.

Appendix

Table 14.8-Bus Unbalanced Three-Phase System Data

Slack Bus (Voltage Setpoint)	1.00 p.u.
Frequency	60 Hz
HV Busbar Voltage	115 kV
LV Busbar Voltage	24.9 kV

Table15. Tranformer Data of the 8-Bus Unbalanced Three-Phase System

Rating	2.5 MVA
Connection (HV/LV)	Delta/G.Wye
Impedance	R=1%, X=8%

Table16. Load Data of the 8-Bus Unbalanced Three-Phase System (in KW and KVAR)

Load	Phase A		Phase B		Phase C	
	P	Q	P	Q	P	Q
C. Power	0	0	30	15	25	14
C. Current	0	0	16	8	0	0
C. Power	20	16	20	16	20	16
C. Current	9	7	9	7	9	7
C. Imped.	135	108	135	108	135	108

Table17. 2-Bus Balanced Three-Phase System Data

Slack Bus (Voltage Setpoint)	1.04 p.u.
Frequency	60 Hz
Busbar Voltage	230 kV
Line Impedance	R=8.993 Ohm/km X= 48.668 Ohm/km
Susceptance	298.69 uS/km
Length of the line	1 km
Load	P=90 MW, Q=30 MVAR

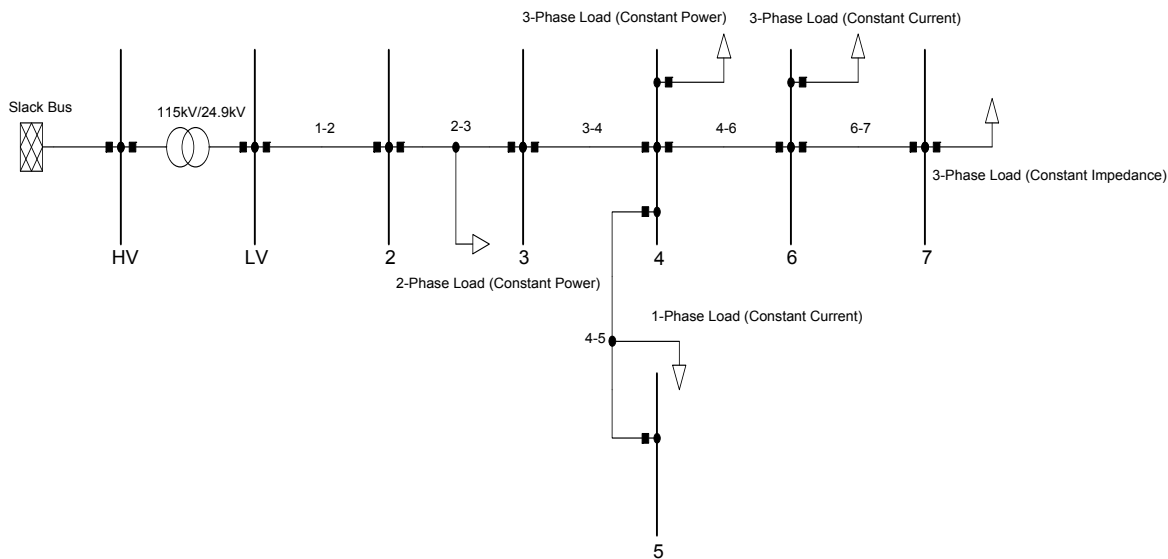


Fig.21. 8-bus unbalanced three-phase system

### REFERENCES

- [1] Claudio A. Canirez, Sameh K. M. Kodsi, Tool for Voltage Collapse Assessment, *IEEE Conference on Mediterranean Electrotechnical-MELECON2006*~May16-19, (2006), Benalmadena, Spain.
- [2] Claudia Reis, Antonio Andrade, F. P. Maciel, Voltage Stability Analysis of Electrical Power System, *International Conference on Power Engineering, Energy and Electrical Drives-POWERENG 2009*~March 18-20, 2009, Lisbon, Portugal.
- [3] Yuanning Wang, Wilsun Xu, The Existence of Multiple Power Flow Solutions in Unbalanced Three Phase Circuits, *IEEE Trans. Power Systems*, vol. 18 n. 2, May 2003, pp. 605-610.
- [4] Mamdouh Abdel-Akher, Mahrous E. Ahmad, Rabindra N. Mahanty, Khalid Mohamed Nor, An Approach to Determine a Pair of Power-Flow Solutions Related to the Voltage Stability of Unbalanced Three-Phase Networks, *IEEE Transactions on Power Systems*, vol. 23 n. 3, Aug. 2008, pp. 1249-1257.
- [5] Xiao-Ping Zhang, Ping Ju, Edmund Handschin, Continuation Three-Phase Power Flow: A Tool for Voltage Stability Analysis of Unbalanced Three-Phase Power Systems, *IEEE Transactions on Power Systems*, vol. 2 n. 3, August 2005, pp. 1320 - 1329.
- [6] Xiao-Ping Zhang, Continuation Power Flow in Distribution System Analysis, *Conference and Exposition on Power Systems-PSCE 2006*~, October 29-November 1, 2006, Georgia, USA.
- [7] Juan M. Ramirez, Jose L. Murillo-Perez, Steady-State Voltage Stability With StatCom, *IEEE Transactions on Power Systems*, vol. 21 n. 3, August 2006, pp. 1453-1454.
- [8] G. Carpinelli, D. Lauria, P. Varilone, Voltage stability analysis in unbalanced power systems by optimal power flow, *IEE Proc. Generation, Transmission and Distribution*, vol. 153 n. 3, May 2006, pp. 261-268.
- [9] Sugunesan Gunalan, Agileswari K. Ramasamy and Renuga Verayiah, Impact of Static Load on Voltage Stability of an Unbalanced Distribution System, *International IEEE Conference on Power and Energy-PECON 2010*~ November 29-December 1, 2010, Kuala Lumpur, Malaysia.
- [10] IEEE Radial Test Feeders [Online]. Available: <http://ewh.ieee.org/soc/pes/dsacom/testfeeders/index.html>
- [11] Yuan Zhou, Venkataramana Ajarapu, A Fast Algorithm for Identification and Tracing of Voltage and Oscillatory Stability Margin Boundaries," in *Proceedings of the IEEE*, vol. 93 no. 5, May 2005, pp. 934-946.
- [12] Nima Amjadi, Mohammad Hossein Velayati, Evaluation of the maximum loadability point of power systems considering the effect of static load models, *Elsevier Energy Conversion and Management*, vol. 50 n.12, Dec. 2009, pp. 3202-3210.
- [13] Jia Hongjie, Yu Xiaodan, Yu Yixin, An improved voltage stability index and its application, *Elsevier Electric Power and Energy Systems*, vol. 27 n.8, Oct. 2005, pp. 567-574.
- [14] Prabha Kundur, *Power System Stability and Control* (McGraw-Hill, Inc., 1994).
- [15] P.K. Modi, S.P. Singh, J.D. Sharma, Fuzzy neural network based voltage stability evaluation of power systems with SVC, *Elsevier Applied Soft Computing*, vol. 8 n.1, Jan. 2008, pp. 657-665.
- [16] PSAT Software Package [Online]. Available: <http://www.power.uwaterloo.ca/~fmilano/psat.htm>
- [17] Badrul H. Chowdhury, Carson W. Taylor, Voltage Stability Analysis: V-Q Power Flow Simulation Versus Dynamic Simulation, *IEEE Transactions on Power Systems*, vol. 15 n.4, Nov. 2000, pp. 1354-1359.